

## Photoemission from bulk bands along the surface normal of W(110)

J. Feydt, A. Elbe, H. Engelhard, and G. Meister

*Fachbereich Physik, Universität Kassel, Heinrich-Plett-Strasse 40, D-34132 Kassel, Germany*

Ch. Jung

*BESSY-GmbH, Lentzeallee 100, D-14195 Berlin, Germany*

A. Goldmann

*Fachbereich Physik, Universität Kassel, Heinrich-Plett-Strasse 40, D-34132 Kassel, Germany*

(Received 20 April 1998)

Normal-emission photoelectron spectra were recorded from W(110) using photons in the energy-range  $11 \text{ eV} \leq \hbar\omega \leq 30 \text{ eV}$ . The results are discussed in comparison to available band-structure calculations and experimental data obtained in earlier studies. We find reasonable overall agreement and summarize a set of “best” critical-point energies along the  $\Gamma$ - $\Sigma$ - $N$  direction of the bulk Brillouin zone, both below and above the Fermi energy. [S0163-1829(98)03144-0]

### I. INTRODUCTION

The investigation of the electronic properties of tungsten by electron spectroscopies has a long history.<sup>1-17</sup> Since the “classical” work of Feuerbacher and Christensen<sup>1-3</sup> several groups have studied the (100), (110), and (111) surfaces employing various angle-resolved experimental methods like ultraviolet valence-band photoemission,<sup>4,5,12,14</sup> inverse uv photoemission,<sup>10,16,17</sup> secondary electron emission,<sup>5,7</sup> x-ray-induced valence-band photoemission,<sup>6,9</sup> and surface core-level spectroscopy using synchrotron radiation at high resolution.<sup>11,13,15</sup> While valence-band studies of W(100) observe<sup>4</sup> reasonable agreement with the available fully relativistic band-structure calculation of Christensen,<sup>2</sup> to our knowledge no mapping of the occupied bulk energy bands  $E(\mathbf{k})$  in their dependence on electron wave vector  $\mathbf{k}$  has ever been reported. In fact the interpretation of the angle-resolved spectra appears complicated<sup>3</sup> by the superposition of different contributions to the electron energy distribution, like bulk direct transitions, features reminiscent of the one-dimensional density of states along the probed  $k_{\parallel}$  (the component of  $\mathbf{k}$  parallel to the surface), secondary electron emission from bands above the vacuum level  $E_v$ , and (sometimes very dominant) emission out of two-dimensional surface states or surface resonances. Moreover, significant contributions of phonon-assisted indirect bulk transitions gaining relevance at increasing photon energies have been reported.<sup>6,9</sup> Finally, an anomalous broadening of photoemission linewidths on W(110) due to creation of phonons during the photoexcitation process has been discussed.<sup>20</sup> By these various effects it is very difficult, and sometimes obviously impossible, to perform a straightforward band mapping experiment as, e.g., easily done for metals like copper<sup>18</sup> or gold.<sup>19</sup> In conclusion photoemission from the low-index surfaces of tungsten is not well understood.

W(110) is an experimentally convenient substrate for the epitaxial growth of several metals and metal alloys. We have recently started a systematic study of such growth processes and of the interaction of the adlayers with gaseous adsorbates

using angle-resolved photoelectron spectroscopy. In this context we need a rather detailed understanding of the clean substrate emission features from bands below  $E_F$ . However, the available results are not easily understood. Most of the existing data from clean W(110) do not show a clear band dispersion with  $k_{\perp}$ ,<sup>8,12,17</sup> and were considered to be representative of the one-dimensional density of states.<sup>8</sup> Also an intense surface resonance peak is observed in normal emission at an initial state energy  $E_i = -1.2 \text{ eV}$  (Ref. 12) below  $E_F$ , which is explained as a surface state supported by a symmetry pseudogap.<sup>12</sup> The absence of clear bulk band dispersion could be due to multiple upper bands or evanescent states in extended bulk band final-state gaps. Earlier work on variable photon energies had been reported at  $\hbar\omega < 12 \text{ eV}$  (Ref. 3) and  $\hbar\omega = 20 \dots 50 \text{ eV}$ .<sup>8</sup> We have therefore performed an investigation of normal emission from W(110) which concentrates on photon energies between 12 and 30 eV. Our results are in essential agreement with the calculated bulk band structure of Christensen.<sup>2</sup> In the following we report our experiments and summarize a set of critical point energies along the  $\Gamma$ - $\Sigma$ - $N$  direction, both below and above the Fermi energy  $E_F$ .

### II. EXPERIMENTAL

The W(110) crystal is oriented to  $\pm 0.25^\circ$ . It is 1.5 mm thick and has a diameter of about 10 mm. It is mounted between two tungsten rods and may be heated from the rear by electron bombardment. Cleaning proceeds by heating in an oxygen atmosphere ( $5 \times 10^{-8}$  Torr) at a temperature of  $T = 1400 \text{ K}$  and a subsequent flash to  $T = 2300 \text{ K}$ . This preparation was found adequate by the absence of contamination as checked by core-level photoelectron spectroscopy, a very sharp pattern of low-energy electron diffraction spots showing no residuals of carbon overlayers, and (perhaps most important) a very sharp surface resonance<sup>12</sup> at  $E_i = -1.2 \text{ eV}$ . In fact we periodically checked for the intensity of this resonance to monitor sample contamination from the residual pressure in the experimental chamber (base pressure

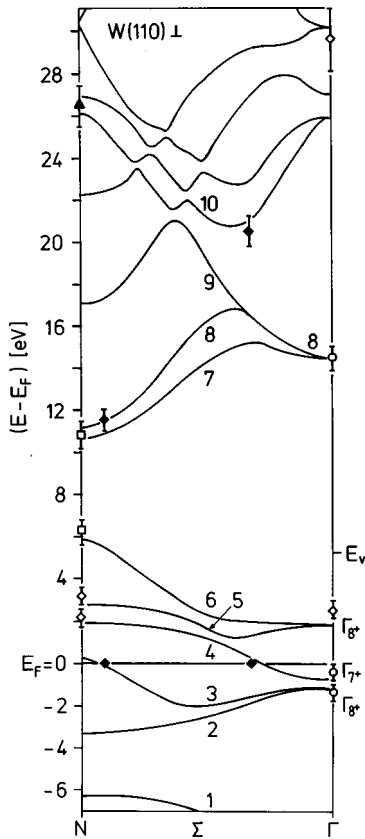


FIG. 1. Electronic energy band structure of tungsten along the  $\Gamma$ - $\Sigma$ - $N$  symmetry direction of the bulk Brillouin zone as calculated by Christensen (Refs. 2, 5) using a relativistic augmented-plane-wave (RAPW) method.  $E_v$  indicates the position of the vacuum level at the W(110) surface. Critical point energies obtained experimentally by different groups are shown by open symbols. Filled symbols localize direct transitions along  $\Sigma$  observed in angle-resolved inverse photoelectron spectroscopy. For details see text.

$8 \times 10^{-11}$  Torr). If necessary, adsorbates could be removed by short heating to  $T = 2300$  K.

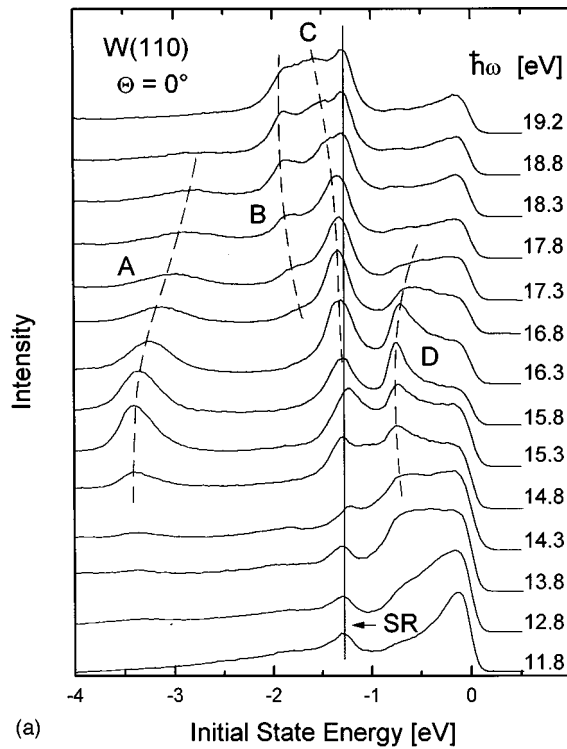
Normal emission photoelectron spectra were taken using the 3 m normal-incidence-monochromator NIM1 (beamline 33.21) at the Berlin electron storage ring BESSY. Electrons were detected with a hemispherical energy analyzer of 152 mm radius of curvature. Its electrostatic input lens is equipped with an aperture that may be changed *in situ* to obtain a continuous variation of the angular resolution between  $\Delta\theta = \pm 1^\circ$  and  $\pm 12^\circ$ . Most data were taken at  $\Delta\theta = \pm 2^\circ$ . The analyzer energy resolution as defined by the pass energy may be varied between  $\Delta E_a = 20$  and 200 meV. If not specified differently the electron distribution curves were taken at a total resolution  $\Delta E = 80$ –100 meV including the contribution from the monochromator. The photons are about 90%  $p$  polarized and are incident at  $60^\circ$  with respect to the surface normal. The vector potential  $\mathbf{A}$  of the photon field was oriented parallel to the  $\Gamma$ NPH mirror plane of the bulk Brillouin zone (i.e., the  $\bar{\Gamma}$ - $\bar{\Sigma}$ - $\bar{H}$  direction of the surface Brillouin zone).

### III. RESULTS AND DISCUSSION

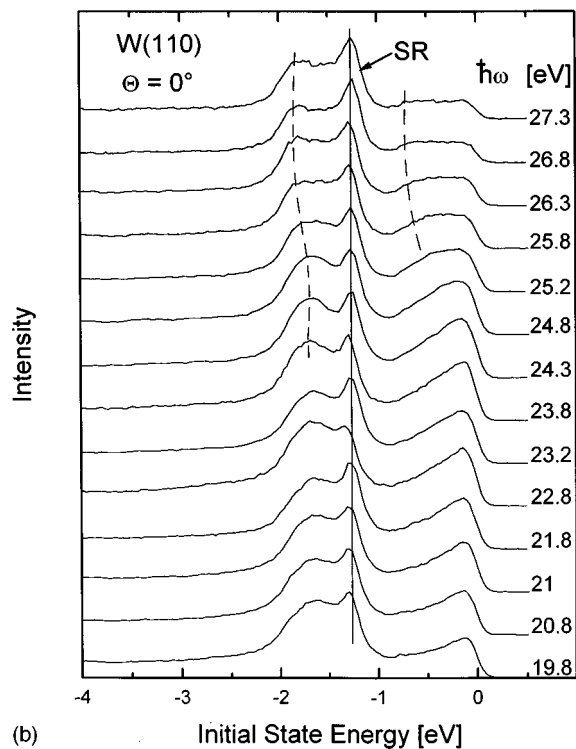
Figure 1 reproduces the bulk band structure as calculated by Christensen<sup>2,3,5</sup> along the  $\Gamma$ - $\Sigma$ - $N$  direction of the bulk

Brillouin zone. Also included are some experimental data. Smith *et al.*<sup>4</sup> studied normal photoemission from W(001), i.e., from bands along  $\Gamma$ - $\Delta$ - $H$ . They report that all major features observed with normally incident  $s$ -polarized radiation ( $10 \text{ eV} \leq \hbar\omega \leq 30 \text{ eV}$ ) agree well with the calculated band structure. At  $\Gamma$  they derived critical point energies at<sup>4</sup>  $E_i \approx -0.4 \text{ eV}(\Gamma_7^+)$ ,  $E_i \approx -1.3 \text{ eV}(\Gamma_8^+)$  and  $E_f = +14.6 \text{ eV}$ . These are shown as open circles in Fig. 1. Willis and Christensen<sup>5</sup> and Schäfer *et al.*<sup>7</sup> measured angle-resolved energy distribution of secondary electron emitted from the unoccupied bands of low-index tungsten surfaces and found good agreement with the calculated bands. From Fig. 3 of Ref. 5 we extract final-state energies of  $E_f = 6.3 \text{ eV}$  and  $E_f = 10.8 \text{ eV}$  (both with an error of about  $\pm 0.5 \text{ eV}$  as estimated by us). These were interpreted<sup>5</sup> as critical point energies around  $N$  and are shown in Fig. 1 by open squares. Blanchet *et al.*<sup>8</sup> observed normal emission photoelectrons from W(110) for photon energies between 24 and 50 eV. They observe that the major peaks in the spectra do not show any resolved dispersion. They conclude that these features are not due to direct transitions between bulk bands but most probably originate from two-dimensional electronic states near the surface. However they also report a dramatic intensity variation with  $\hbar\omega$ , presumably due to the final states in the excitation process.<sup>8</sup> We come back to this aspect further below. Finally the unoccupied bands of W(110) were probed by inverse photoemission.<sup>17</sup> Critical point energies are determined to be at  $E_f = +2.6 \text{ eV}$  ( $\Gamma_8^+$ , or  $\Gamma_{12}$  in the nonrelativistic point-group notation if spin-orbit coupling is neglected),  $E_f = +2.2 \text{ eV}$  and  $E_f \geq +3.2 \text{ eV}$  (both at  $N$ ). These data are shown in Fig. 1 by open diamonds. Moreover, these authors observed the energies of direct transitions to the two Fermi-level crossing points (shown by filled diamonds in Fig. 1), which were known to occur at wave vectors  $k_\perp$  of 0.09 ( $N\Gamma$ ) and 0.67 ( $N\Gamma$ ) from existing de Haas-van Alphen data. This knowledge allows us to locate also the initial states of the normal-incidence spectra along  $\Gamma N$ , see the filled diamonds at  $E_f = +11.5 \text{ eV}$  and  $E_f = +20.5 \text{ eV}$  in Fig. 1. In conclusion the earlier studies strongly support details of the calculated final-state bands along  $\Gamma$ - $\Sigma$ - $N$ . We will therefore use this knowledge in the interpretation of our study of the bulk bands below  $E_F$ .

Inspection of Fig. 1 shows a large gap between about 6 and 11 eV above  $E_F$ , which does not allow bulk direct transitions to occur along  $\Gamma$ - $N$ . In consequence strong damping effects due to a large imaginary part of the potential will occur. Damping results in a short mean free path of the electrons emitted along the surface normal and therefore (while  $k_\parallel$  remains a good number)  $k_\perp$  gets unsharp. We must therefore expect considerable integration over  $k_\perp$  along  $\Gamma$ - $\Sigma$ - $N$ . In consequence normal emission spectra will show some resemblance with the one-dimensional ( $k_\parallel$  resolved) density of states. However, Fig. 1 also shows bands like the ones connecting  $N$  (at  $E_f \approx 11 \text{ eV}$ ) and  $\Gamma$  (at  $E_f = 14.5 \text{ eV}$ ), which may support bulk direct transitions and we know that these will exhibit dispersion with  $k_\perp$ . In fact all the expectations are observed in our results. Figure 2 shows a sample set of normal emission spectra taken at different photon energies. The straight solid line connects photoemission peaks without dispersion, while direct transition features are connected by



(a)



(b)

FIG. 2. Normal emission photoelectron energy distribution curves taken at different photon energies  $\hbar\omega$ : (a) Photon energies between 11.8 and 19.2 eV. (b) Photon energies from 19.8 to 27.3 eV. All spectra are normalized to equal maximum peak amplitude and shifted vertically against each other.

dashed lines. The nondispersing peak at  $E_i = -1.2$  eV has been carefully investigated by Gaylord and Kevan.<sup>12</sup> It was convincingly interpreted by emission from a surface resonance, and this interpretation is strongly supported by our results, see further below. Comparison with Fig. 1 clearly

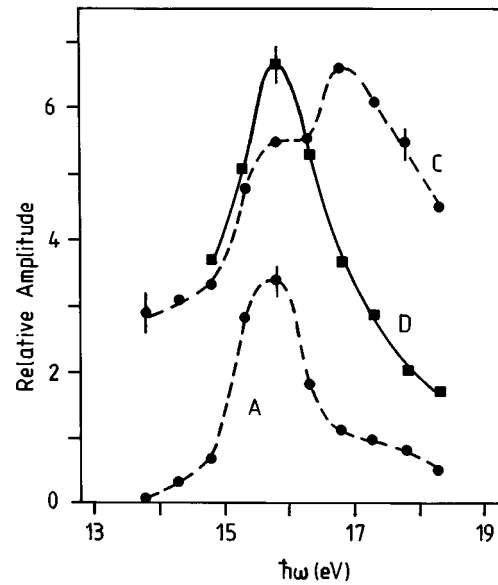


FIG. 3. Relative variation of peak amplitudes of several dispersing features [labeled A, C, and D in Fig. 2(a)] with photon energy  $\hbar\omega$ .

explains the dispersing feature labeled A in Fig. 2(a) by direct transitions between the bands labeled 2 and 8 in Fig. 1. Peaks labeled B (D) result from transitions around  $\Gamma$  between bands 3 (4) and 8.

A more detailed interpretation requires inspection of transition-matrix elements and the underlying selection rules. In the limit of neglected spin-orbit coupling, the electron states along  $\Gamma N$  are subjected to the  $C_{2v}$  point-group symmetry. In this limit very effective selection rules<sup>22-24</sup> couple initial states of symmetries  $\Sigma_1$ ,  $\Sigma_3$ , and  $\Sigma_4$  exclusively to final states of symmetry  $\Sigma_1$ . Only the latter ones are totally symmetric with respect to all point-group operations along the surface normal and therefore contribute exclusively to normal emission spectra.<sup>22</sup> However, for a material like tungsten spin-orbit interaction must not be neglected. In the relativistic double-group notation<sup>25,26</sup> which takes into account the effects of spin-orbit coupling, all states along  $\Gamma N$  belong to the same representation  $\Sigma_5$ . However, this does not prevent several bands to exhibit a predominant orbital character according to the nonrelativistic case: some final-state bands are still dominated by the (former)  $\Sigma_1$  symmetry, which means that not much different character is mixed in by spin-orbit interaction (although, in principle, allowed by symmetry arguments). A detailed analysis of the orbital composition of the final states of Fig. 1 shows<sup>27</sup> that in particular band 8 exhibits essentially  $\Sigma_1$  character. This band will therefore contribute intense direct transition lines.

The onset of the direct transition labeled A in Fig. 2(a) between bands 2 and 8 near the  $N$  point, is also clearly recognized in Fig. 3 where we have plotted the variation of peak intensities with photon energy  $\hbar\omega$ . Since it is not trivial to normalize photoemission spectra to the photon flux, we have applied a simplified procedure: A linear background intensity is defined for peak A in Fig. 2(a). Figure 3 now shows the amplitude at maximum of peaks A, B, C divided by the background amplitude below peak A. This procedure appears justified by the monotonic and almost constant photon flux pro-

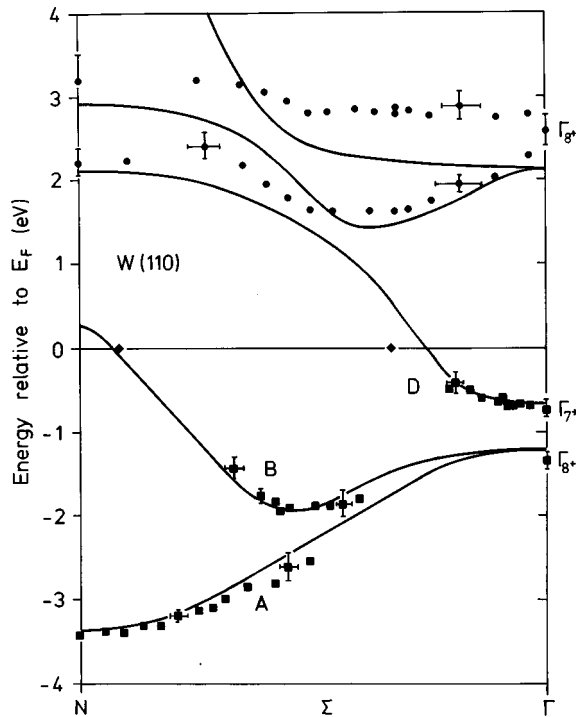


FIG. 4. Occupied and unoccupied band dispersion along  $\Gamma$ - $\Sigma$ - $N$  of W(110), derived from inverse photoemission spectra [circles (Ref. 17)] and normal emission photoelectrons (squares, this work). The relativistic band calculation of Christensen (Ref. 2) is given by the solid lines for comparison. The diamonds are from de Haas-van Alphen data (Ref. 17).

duced by the monochromator in the considered range of photon energies. We have also tried different normalizations to secondary electron background: while the detailed shape of the intensity variation changes, the pronounced maxima observed in Fig. 3 are independent of the applied normalization procedures. Peak A has its maximum at  $\hbar\omega = 15.7$  eV, while peak D resonates at  $\hbar\omega = 15.9$  eV. Inspection of Fig. 1 explains peak D by a transition from  $\Gamma_{7+}$  at  $E_i = -0.75$  eV to band 8 at  $\Gamma$ . The calculated band 8 meets  $\Gamma$  at  $E_f = 14.5$  eV and this predicts an allowed direct transition at  $\hbar\omega = 15.2$  eV, i.e., only 0.7 eV off the resonance observed for D in Fig. 3. At N, we observe  $E_i = -3.4$  eV and Fig. 1 gives  $E_f = 11.2$  eV for band 8. This predicts a direct transition resonance at  $\hbar\omega \geq 14.6$  eV. These numbers indicate that band 8 should be shifted rigidly by about 0.8 eV to higher final-state energies. This is not unreasonable. First, also the inverse photoemission data,<sup>17</sup> which are shown as open diamonds in Fig. 1, indicate some shift into the same direction. Second it is well known<sup>24,28</sup> that photoemission probes an excited state of the electronic structure, while the one-electron band-structure calculation treats the ground state of the system. Third an energy shift of  $\leq 1$  eV at more than 10 eV above  $E_F$  is well within the expected accuracy of the band calculation.

We have now used this shifted final-state band 8 (and the experimentally observed initial-state energies) to derive values of  $k_{\perp}$  for the dispersing features A, B, and D of Fig. 2(a). The results are summarized as filled squares in Fig. 4. Also shown are the bands as calculated by Christensen,<sup>2</sup> and data points above  $E_F$  (filled circles) obtained from inverse photo-

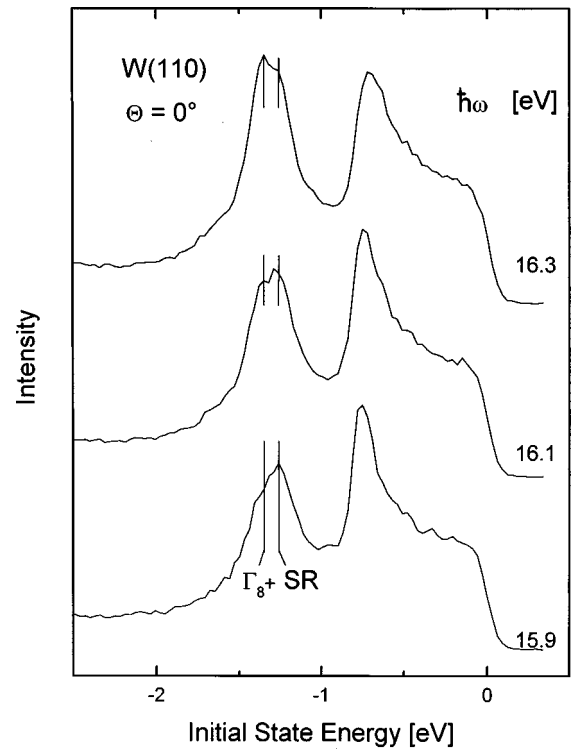


FIG. 5. Normal emission spectra from W(110) indicating the variation of relative peak intensities with photon energy  $\hbar\omega$ , see text for details.

emission spectroscopy.<sup>17</sup> As is obvious from Fig. 4 all occupied bands are described almost perfectly by the calculation, with typical error bars below 0.3 eV in  $E_i$  and less than a few percent of  $k_{\perp}$  on the average. Also above  $E_F$  the observed shifts between experimental and calculated bands never exceed 0.6 eV. A similar good agreement is also reached for other theoretical results: several different types of band calculations, such as the self-consistent relativistic pseudopotential calculation of Bylander and Kleinmann,<sup>29</sup> the semirelativistic linearized augmented-plane-wave (APW) calculations done by Jansen and Freeman<sup>30</sup> and Wei, Krakauer, and Weinert<sup>31</sup> agree with each other and with the relativistic APW calculation of Christensen and Feuerbacher<sup>2</sup> within typically 0.2 eV between the bottom of the valence band and up to several eV above  $E_F$ . We conclude that the bulk bands along  $\Gamma$ - $\Sigma$ - $N$  in tungsten are rather well understood.

Figure 3 indicates a double-peaked intensity variation of the feature labeled C in Fig. 2. Our interpretation is as follows. The intensity producing the plateau observed in Fig. 3 around  $\hbar\omega = 16$  eV is due to a resonant excitation of the surface resonance labeled SR in Fig. 2. The maximum at  $\hbar\omega = 16.6$  eV in Fig. 3 results from the resonant direct transition starting at  $\Gamma_{8+}$ , compare also Fig. 1. High-resolution spectra displayed in Fig. 5 show the development of the different peak intensities. Such data allow us to locate  $\Gamma_{8+}$  at  $E_i = (-1.32 \pm 0.05)$  eV. Already in the work of Blanchet, DiNardo, and Plummer<sup>8</sup> dramatic intensity variations with photon energy were observed. One rather narrow resonance occurs at  $E_i \approx -3.4$  eV around  $\hbar\omega = 30$  eV and we interpret this by a direct transition at the N point. This yields an additional final state point at  $E_f \approx 26.6$  eV which is shown as a

TABLE I. Comparison of experimental and theoretical critical point energies (in eV) at high-symmetry points of the bcc bulk Brillouin zone.

Critical point	Calculations			Experiments	
	Refs. 2, 5	Ref. 29	Energy	Ref.	Other results
$\Gamma_{8+}$	-1.17	-1.53	$-1.32 \pm 0.10$	This work	$\approx -1.3$ (Ref. 4)
$\Gamma_{7+}$	-0.61	-1.01	$-0.75 \pm 0.05$	This work	$\approx -0.4$ (Ref. 4)
$\Gamma_{8+}$	1.99	2.15	$2.6 \pm 0.2$	17	
$\Gamma$	14.4	14.9	$15.3 \pm 0.5$	This work	$\approx 15$ (Ref. 5); $14.6 \pm 0.6$ (Ref. 4)
$\Gamma$	30.2		$29.7 \pm 1.7$	17	
$N_{5+}$	-3.35	-3.66	$-3.40 \pm 0.05$	This work	-3.5 (Ref. 8)
$N_{5+}$	1.96	1.98	$2.2 \pm 0.2$	17	
$N_{5+}$	2.89	2.94	$\geq 3.2$	17	
$N_{5+}$	5.90	5.88	$6.3 \pm 0.5$	5	
$N_{5+}$	10.7	9.97	$10.8 \pm 0.5$	5	
$N_{5-}$	11.1	11.7			
$N$	26.1, 26.9		$\approx 26.5$	8	
$H_{8+}$	-6.1	-5.9	-5.7	4	
$H_{8-}$	9.0	9.2	9.3	4	$\approx 9.5$ (Ref. 5)

filled triangle in Fig. 1. A summary of all available critical point energies, both calculated and obtained experimentally, is given in Table I. The first column of the experimental results shows what we believe to be the set of ‘‘best energies’’ presently available.

All energies collected in Table I agree very well with the calculated bulk band energies, even for final-state energies well above  $E_F$ . Typical energy differences of the experimental bands along  $\Gamma$ - $\Sigma$ - $N$  are  $\Delta E_i \leq 0.2$  eV, and the electron wave vectors are reproduced with an accuracy of  $\Delta k_{\perp} < 0.1 \text{ \AA}^{-1}$  which corresponds to  $\leq 7\%$  of the distance between  $N$  and  $\Gamma$ . Whenever bulk final-state bands appropriate for bulk direct transitions are available, such transitions are observed in the normal emission spectra. If broad gaps open above  $E_F$ ,  $k_{\perp}$  is heavily broadened as is expected, and the electron distribution curves represent an integration over the extended  $k_{\perp}$  regions along  $\Gamma N$ , while  $k_{\parallel}$  is still conserved (we have checked this by taking spectra at polar angles slightly off normal—these differ drastically from the ones shown in Fig. 2). Such integration occurs at photon energies  $\hbar\omega < 15$  eV and, in particular, at  $\hbar\omega = 20$ – $30$  eV [compare Fig. 2(b)]. In the latter case integration is caused mainly by the appearance of multiple final states at  $E_f > 20$  eV, compare Fig. 1: all contribute to a certain extent and most probably the resulting superposition washes out the individually dispersing features. In consequence the resulting electron distribution curves exhibit (some) resemblance to the one-dimensional density of states along  $\Gamma N$  ( $k_{\parallel} = 0$ ). Since the integration along  $k_{\perp}$  is incomplete, however, there are still

some features changing with  $\hbar\omega$ , see for example in Fig. 2(b) the broad shoulder dispersing from  $E_i \approx -1.7$  eV at  $\hbar\omega = 21$  eV to  $\approx -1.9$  eV at  $\hbar\omega = 27$  eV. At the same photon energies the broad feature from  $E_F$  to about  $-0.7$  eV still shows some movement between  $\hbar\omega = 24$  and  $27.5$  eV.

In conclusion all data collected in the present work are consistent with the bulk band structure as calculated for bcc tungsten. Therefore we see no need to consider (with the exception of the surface resonance at  $E_i = -1.2$  eV) emission from a surface density of states that differs from what we expect from the bulk bands. In particular there is no evidence for a narrowing of the  $d$  bands at the surface,<sup>3</sup> i.e., for a shift of the gap positions between the bulk and the surface electron density of states. In fact we would not expect a surface that differs electronically very much from the bulk: a recent structural study presents convincing evidence that the W(110) surface does not reconstruct, but only the first interlayer distance is contracted by about 3% as compared to the bulk.<sup>21</sup> This contraction is sufficient to split-off a surface resonance from a bulk band, but cannot change the electronic properties over larger areas of the surface Brillouin zone.

#### ACKNOWLEDGMENTS

This work was supported by the Bundesministerium für Bildung und Forschung (BMBF). We thank W. Braun and the BESSY staff for help. A.E. acknowledges a generous grant from the ‘‘Otto-Braun-Stiftung.’’

<sup>1</sup>B. Feuerbacher and B. Fitton, Phys. Rev. Lett. **30**, 923 (1973).

<sup>2</sup>N. E. Christensen and B. Feuerbacher, Phys. Rev. B **10**, 2349 (1974).

<sup>3</sup>B. Feuerbacher and N. E. Christensen, Phys. Rev. B **10**, 2373 (1974).

<sup>4</sup>R. J. Smith, J. Anderson, J. Hermanson, and G. J. Lapeyre, Solid State Commun. **19**, 975 (1976).

<sup>5</sup>R. F. Willis and N. E. Christensen, Phys. Rev. B **18**, 5140 (1978).

<sup>6</sup>Z. Hussain, C. S. Fadley, S. Kono, and L. F. Wagner, Phys. Rev. B **22**, 3750 (1980).

- <sup>7</sup>J. Schäfer, R. Schoppe, J. Hölzl, and R. Feder, *Surf. Sci.* **107**, 290 (1981).
- <sup>8</sup>G. B. Blanchet, N. J. DiNardo, and E. W. Plummer, *Surf. Sci.* **118**, 496 (1982).
- <sup>9</sup>R. C. White, C. S. Fadley, M. Sagurton, and Z. Hussain, *Phys. Rev. B* **34**, 5226 (1986).
- <sup>10</sup>W. Drube, D. Straub, F. J. Himpsel, P. Soukassian, C. L. Fu, and A. J. Freeman, *Phys. Rev. B* **34**, 8989 (1986).
- <sup>11</sup>Y. Jugnet, N. S. Prakash, Tran Minh Duc, H. C. Poon, G. Grenet, and J. B. Pendry, *Surf. Sci.* **189/190**, 782 (1987).
- <sup>12</sup>R. H. Gaylord and S. D. Kevan, *Phys. Rev. B* **36**, 9337 (1987).
- <sup>13</sup>G. K. Wertheim and P. H. Citrin, *Phys. Rev. B* **38**, 7820 (1988).
- <sup>14</sup>R. H. Gaylord, K. Jeong, S. Dhar, and S. D. Kevan, *J. Vac. Sci. Technol. A* **7**, 2203 (1989).
- <sup>15</sup>D. M. Riffe, G. K. Wertheim, P. H. Citrin, and D. N. E. Buchanan, *Phys. Scr.* **41**, 1009 (1990).
- <sup>16</sup>I. R. Collins, A. D. Laine, P. T. Andrews, and P. J. Durham, *J. Phys.: Condens. Matter* **3**, 5307 (1991).
- <sup>17</sup>Dongqi Li, P. A. Dowben, J. E. Ortega, and F. J. Himpsel, *Phys. Rev. B* **47**, 12 895 (1993).
- <sup>18</sup>R. Courths and S. Hüfner, *Phys. Rep.* **112**, 53 (1984).
- <sup>19</sup>R. Courths, H.-G. Zimmer, A. Goldmann, and H. Saalfeld, *Phys. Rev. B* **34**, 3577 (1986).
- <sup>20</sup>S. Dhar and S. D. Kevan, *Phys. Rev. B* **41**, 8516 (1990).
- <sup>21</sup>M. Arnold, G. Hupfauer, P. Bayer, L. Hammer, K. Heinz, B. Kohler, and M. Scheffler, *Surf. Sci.* **382**, 288 (1997).
- <sup>22</sup>J. Hermanson, *Solid State Commun.* **22**, 9 (1977).
- <sup>23</sup>W. Eberhardt and F. J. Himpsel, *Phys. Rev. B* **21**, 5572 (1980).
- <sup>24</sup>S. Hüfner, *Photoelectron Spectroscopy—Principles and Applications*, Springer Series in Solid State Science, Vol. 82 (Springer, Berlin, 1995).
- <sup>25</sup>G. Borstel, W. Braun, M. Neumann, and G. Seitz, *Phys. Status Solidi B* **95**, 453 (1979).
- <sup>26</sup>G. Borstel, M. Neumann, and G. Wöhlecke, *Phys. Rev. B* **23**, 3121 (1981).
- <sup>27</sup>J. Noffke (private communication).
- <sup>28</sup>*Angle-Resolved Photoemission, Theory and Current Applications*, edited by S. D. Kevan (Elsevier, Amsterdam, 1992).
- <sup>29</sup>D. M. Bylander and L. Kleinmann, *Phys. Rev. B* **29**, 1534 (1984).
- <sup>30</sup>H. J. F. Jansen and A. J. Freeman, *Phys. Rev. B* **30**, 561 (1984).
- <sup>31</sup>S.-H. Wei, H. Krakauer, and M. Weinert, *Phys. Rev. B* **32**, 7792 (1985).